ELSEVIER

Journal of Fluorine Chemistry 110 (2001) 165–173

JOURNAL OF FLUORINE CHEMISTRY

www.elsevier.com/locate/jfluchem

Review

Fluoride glass compositions for waveguide applications

G. Rault, J.L. Adam*, F. Smektala, J. Lucas

Laboratoire des Verres et Céramiques, UMR-CNRS 6512, Université de Rennes 1, Campus de Beaulieu, 35042 Rennes Cedex, France

Received 27 December 2000; accepted 7 February 2001

Abstract

Compositions along with thermal and optical properties of fluoride glasses suitable for the preparation of fibers and planar waveguides are reviewed. In terms of application, emphasis is given on the characteristics of Tm^{3+} and Pr^{3+}-doped ZrF_4-based fluoride glasses for optical amplification at 1.47 and 1.3 μm.

Then, experimental results on the optimization of indium-based fluoride glasses are shown. Glasses are investigated in the (Ba, In, Zn, Gd) and (In, Zn, Sr, Ba) fluoride systems. Optical fibers are pulled from glasses of the (In, Zn, Sr, Ba) system stabilized with addition of gallium and calcium fluorides.

Keywords: Glass; Indium fluoride; Fiber; Rare-earth; Optical amplification

1. Introduction

Fluoride glasses (FG) have been studied since the middle of the seventies essentially because of their potential for applications in optical telecommunication [1,2]. FG such as zirconium fluoride-based glasses, show a good ability for fiber-drawing [3] which is of prime importance for communication systems. In addition, because of a broader infrared transparency window, FG fibers exhibit theoretical optical losses lower than that of silica fibers [4]. However, the ultra-low-loss level has never been achieved experimentally with FG, which prevents them from applications as long-haul telecommunication fibers [5].

The recent need for optical fiber amplifiers [6,7], to replace electronic regenerators in optical communication, provides a new challenge for FG. These materials possess the potential to surpass rare-earth (RE)-doped silica whose spectral domain for amplification is limited to 1.53–1.60 μm. Thus, due to their low multiphonon emission rates, FG doped with Pr^{3+} or Tm^{3+} ions give rise to emissions at 1.3 and 1.47 μm, respectively. Signal in these wavelength domains, which still belong to the low loss region of telecommunication fibers, cannot be amplified by RE-doped silica fibers.

This paper reviews the optical properties of standard FG suitable for RE-doped optical fibers and planar waveguides, in connection with optical amplification. Recent developments on the composition and thermal properties of indium-based FG are presented as well.

2. Fluoride glasses for optical fiber and planar waveguide: state of the art

FG represent a large family of glassy materials which can be classified by their chemical composition. Three of them are listed in Table 1. They are characterized in terms of the glass transition temperature (T_g), the temperature of crystallization (T_x), the melting temperature (T_m) and the refractive index (n_D) measured at sodium D-line. Glass stability can be estimated by the ΔT parameter, equal to ($T_x - T_g$), which must be as large as possible.

First are the fluorozirconates like ZBLAN or ZBLA glasses. They are based essentially on zirconium fluoride in association with barium, lanthanum, aluminum and, possibly, sodium fluorides. With a ($T_x - T_g$) temperature difference of 90°C and a small crystallization enthalpy, ZBLAN glass is very stable against devitrification. ZBLAN is consequently the material of reference for making FG optical fibers. ZBLA on the other hand is well-suited for the preparation of planar waveguides by F^-/Cl^- ion exchange. The substitution of chlorine ions for less-polarizable fluorine ions results in an increase of the refractive index. Associated with photolithography processes, this method permits the fabrication of channel waveguides, single-mode at 830 and 1015 nm [8].

* Corresponding author. Tel.: +33-299-286-262; fax: +33-299-281-600.
E-mail address: jean-luc.adam@univ-rennes1.fr (J.L. Adam).

0022-1139/01/$ – see front matter
PII: S0022-1139(01)00425-0

Table 1
Composition and physical properties of some typical fluoride glasses

Glass	Composition (mol%)	T_g (°C)	T_x (°C)	T_m (°C)	n_D
ZBLAN	53 ZrF_4–20 BaF_2–4 LaF_3–3 AlF_3–20 NaF	262	352	455	1.498
BIG	30 BaF_2–18 InF_3–12 GaF_3–20 ZnF_2–10 YbF_3–6 ThF_4–4 ZrF_4	332	460	576	1.505
PZG	35.3 PbF_2–23.5 ZnF_2–34.3 GaF_3–4.9 YF_3–2 AlF_3	270	325	547	1.59

The second family concerns fluoroindate glasses such as BIG, which is based on barium, indium and gallium fluorides. These glasses are usually not as stable as ZBLAN, despite a large ($T_x - T_g$) value. This is because the enthalpy of crystallization is larger for InF_3 based glasses. As a consequence, these glasses offer less favorable conditions for fiber-drawing [9,10].

The third one, PZG, is characterized by a high lead content, which results in a high refractive index of 1.59. Not stable enough for fiber-drawing, PZG fluoride glass is on the other hand an appropriate material for realizing channel waveguides by physical vapor deposition. Thanks to similar evolutions of vapor pressure against temperature, lead, zinc and gallium fluorides can be evaporated in a congruent manner and form a FG film by deposition on a CaF_2 substrate [11]. Deposition through a photoresist mask prepared by photolithography leads to single-mode waveguides.

Infrared transmission spectra of silica glass and FG are given in Fig. 1. The infrared cut-off is located at longer wavelength for FG (about 6–7 μm) than for SiO_2 glasses (about 3 μm). This property is directly related to the fundamental vibration modes of the host. Thus, materials with large, heavy and lightly charged elements show the lowest vibration frequencies.

In ZBLAN, the position of the infrared edge at ≈6 μm is due essentially to Zr–F vibrations whose fundamental frequency is at 580 cm^{-1}. In BIG glasses, the vibration modes responsible for the shift of the infrared edge towards longer wavelengths are In–F at 510 cm^{-1} and Ga–F at 570 cm^{-1}. Conversely, high-frequency Si–O vibrations at 1100 cm^{-1} account for the poor infrared transparency of silica limited to 3 μm. Another consequence of low fundamental frequencies is that non-radiative transitions of rare-earth ions are less probable in FG than in silica. This is illustrated in Fig. 2 that shows the multiphonon emission rates of RE ions in silicate and in fluoride glasses as a function of ΔE, the energy gap between the emitting level and the next lower level. Typically, the multiphonon rate is about three orders of magnitude higher in silicates. As a result many transitions, that are inactive in oxide glasses become observable in FG [12]. Similarly, within the FG family, indium-based glasses are better hosts than ZBLAN as far as quantum efficiencies of RE emissions are concerned.

In telecommunication, amplification is needed from 1.3 to 1.6 μm as suggested by the attenuation spectrum of silica fiber in Fig. 3. This can be achieved by using the radiative emissions of Pr^{3+} ions in the 1.3 μm region [9,13,14], Tm^{3+} ions at 1.47 μm [10,13] and well-known Er^{3+} around 1.55 μm.

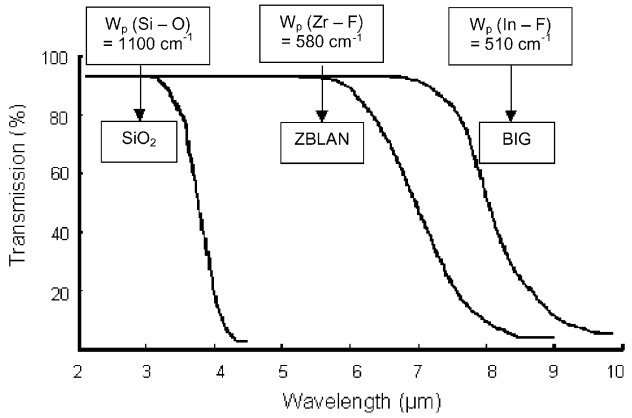

Fig. 1. Infrared transmission spectra of silica glass and fluoride glasses (W_p: fundamental vibrations).

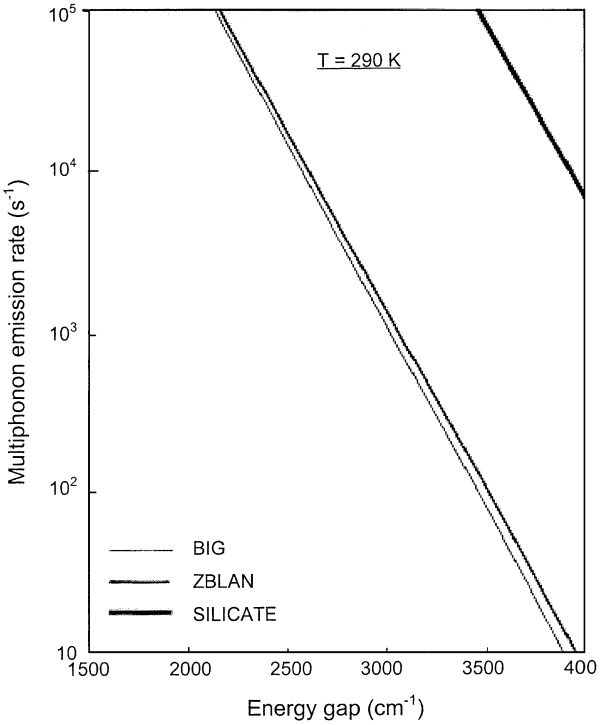

Fig. 2. Multiphonon emission rates of RE ions in silicate and in fluoride glasses [4].

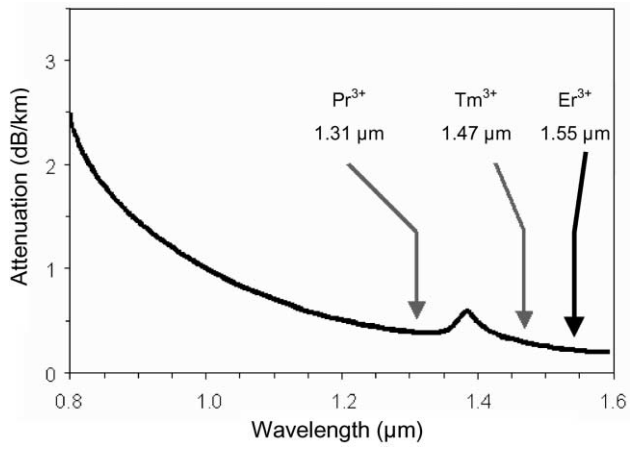

Fig. 3. Attenuation curve of silica fiber. Rare-earth suitable for optical amplification in the minimum-loss region are indicated.

The energy level diagrams of Pr^{3+}, Tm^{3+} and Er^{3+} ions are given in Fig. 4. The 1.3 μm emission of Pr^{3+} takes place from the $^1G_4$ level to $^3H_5$, with direct excitation at 1.02 μm. Because of an energy gap of about 3000 cm^{-1} between $^1G_4$ and its first lower-energy level $^3F_4$, the 1.3 μm radiative emission from $^1G_4$ is totally quenched in Pr^{3+}-doped silica glasses. On the other hand, this transition is possible in lower phonon-energy hosts like FG [15] with a quantum efficiency of about 3% in ZBLAN glass.

The second rare-earth ion showing a valuable transition for telecom applications is Tm^{3+} with emission at 1.47 μm from $^3H_4$ to $^3F_4$. The energy level diagram indicates that the energy gap between $^3H_4$ and $^3H_5$ is around 4500 cm^{-1} which makes this transition more probable in low phonon-energy hosts like FG [16,17]. Efficient pumping is provided by a two-step up-conversion process with 1.064 μm light as described in Fig. 4. Recently, a thulium-doped FG fiber has been implemented as part of a broadband optical amplifier with 17.7 THz range [18].

Er^{3+} ion possess a broad emission band at 1.55 μm due to the $^4I_{13/2}$ to $^4I_{15/2}$ transition.

The large energy gap between $^4I_{13/2}$ and $^4I_{15/2}$ makes non-radiative transitions negligible whatever the host, silica or FG. Erbium-doped silica optical amplifiers have been existing for several years and are commercially available. However, spectral filtering is needed to obtain a flat gain as a function of signal wavelength in these amplifiers [19]. The interest of Er^{3+}-doped FG optical amplifiers is the gain bandwidth which is intrinsically flat from 1530 to 1560 nm. This property is fundamental for wavelength division multiplexing (WDM) applications [13].

3. Development of low phonon InF_3-based glasses

We have conducted research in order to optimize low phonon-energy FG based on InF_3, aiming at materials stable enough to be pulled in optical fibers.

Two different families have been explored. The first one, referred to as BIZ–Gd is based on barium, indium, zinc and gadolinium fluorides. The second one, named IZSB, is based on the $In_{40}Zn_{20}Sr_{20}Ba_{20}F_{240}$ composition [20,21].

3.1. Glasses based on Ba, In, Zn, Gd fluorides

The thermal stability of glass samples was determined by two criteria. The ΔT parameter defined in Section 2, and the shape of the crystallization peak which must be as flat as possible, indicating low kinetics of crystallization.

We first investigated the stabilization of BaF_2–InF_3–ZnF_2 ternary system, referred to as BIZ, by addition of a fourth component, GdF_3. In a previous study, carried out in our laboratory, glass compositions were investigated with a fixed

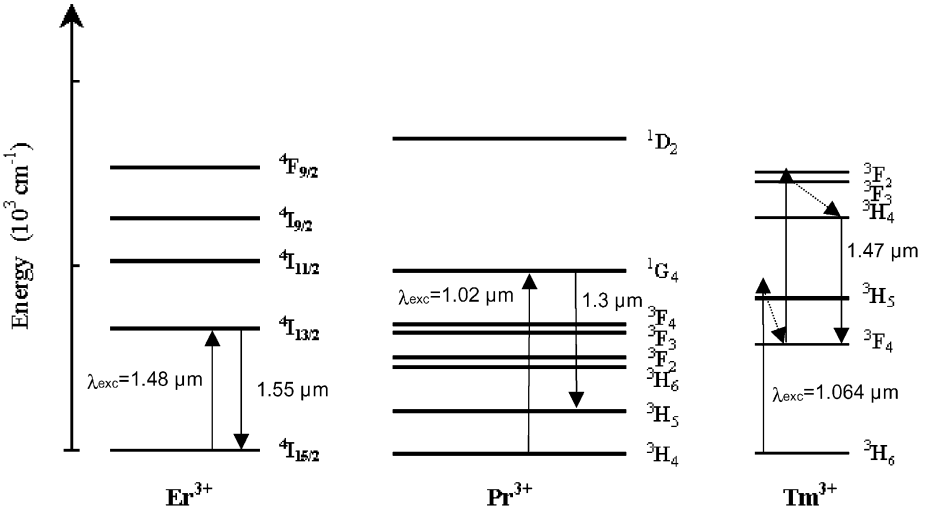

Fig. 4. Partial energy level diagrams of Er^{3+}, Pr^{3+} and Tm^{3+} ions (dashed arrows indicate non-radiative relaxations).

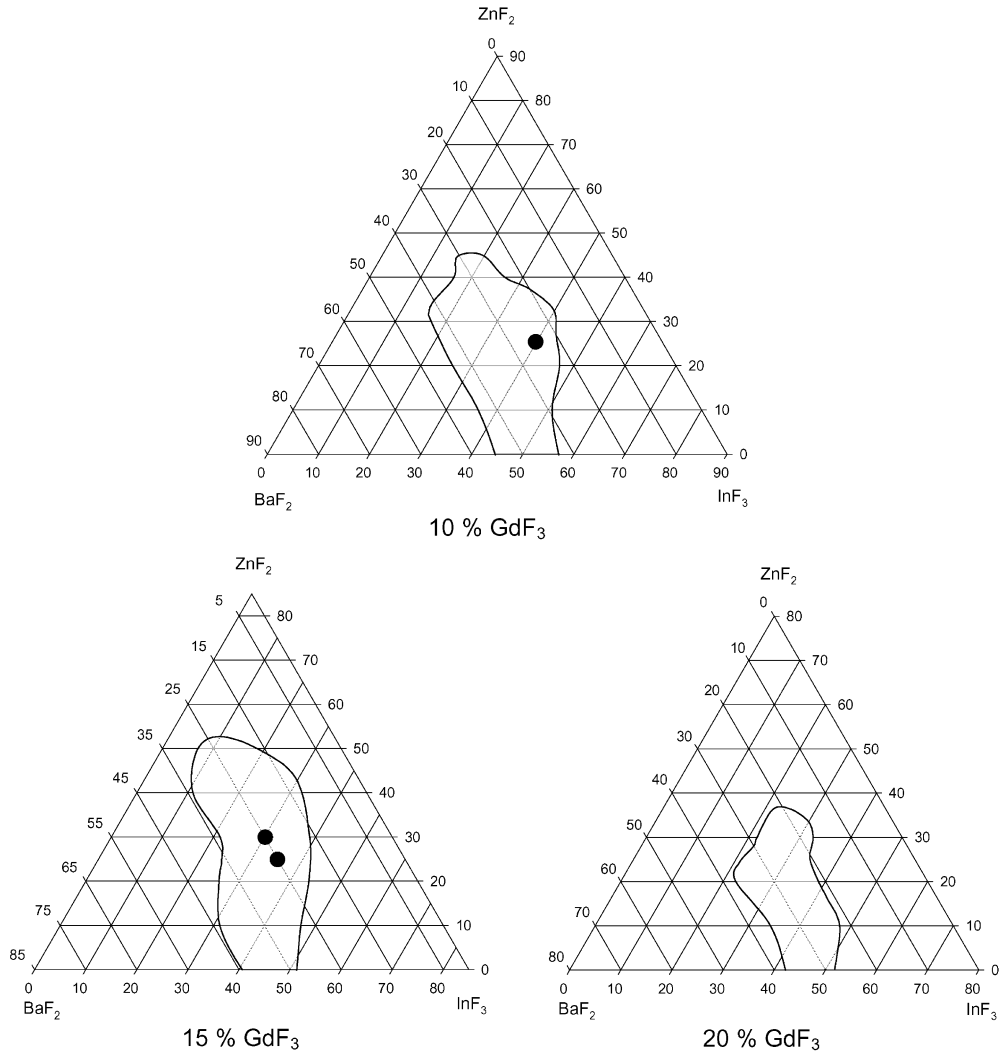

Fig. 5. Vitreous domains in the BaF_2–InF_3–ZnF_2–GdF_3 system with constant GdF_3 concentration of 10, 15 and 20 mol%.

GdF_3 content of 10% [20]. We have confirmed the glassy domain in the BaF_2–InF_3–ZnF_2–10 GdF_3 system and established new glass compositions in the systems containing 15 and 20 mol% GdF_3. The results are shown in Fig. 5, and the limit concentrations of the respective components are listed in Table 2.

Examination of the phase diagrams in that figure reveals that glasses can be formed in the BaF_2–InF_3–GdF_3 system. However, the glassy domain is limited to InF_3 concentrations ranging from ≈40 to 55 mol% with a ΔT stability parameter of about 65°C only. The role of ZnF_2 for glass formation in the Ba–In–Zn–Gd fluoride system is essential, as shown by the expansion of the glassy domains with ZnF_2 concentration.

Two stable glasses have been identified in the 15% GdF_3 diagram. They are shown in Table 3 together with stable compositions containing 10 and 20% GdF_3. According to the respective size of the vitreous domains in Fig. 5, and the ΔT values reported in Table 3, the most stable glasses are likely to contain about 15% of GdF_3. In order to adjust

Table 2
Composition limits in the BaF_2–InF_3–ZnF_2–GdF_3 system with constant GdF_3 concentrations of 10, 15 and 20 mol%

Glass (% GdF_3)	BaF_2	InF_3	ZnF_2
10	18–45	15–58	0–45
15	13–45	8–52	0–52
20	18–38	20–52	0–37

Table 3
Most stable glass compositions in the 10, 15 and 20% GdF_3 vitreous diagram glass composition (mol%)

Glass composition (mol%)				T_g (°C)	T_x (°C)	T_{peak} (°C)	ΔT (°C)
BaF_2	InF_3	ZnF_2	GdF_3				
25	40	25	10	301	389	394	88
25	35	25	15	309	405	408	96
25	30	30	15	311	406	410	95
25	40	15	20	312	398	402	86

further the GdF_3 content, we have carried out additional substitutions according to the following composition laws:

$$25\,BaF_2-(40-x)\,InF_3-25\,ZnF_2-(10+x)\,GdF_3 \quad \text{with } x=0-10 \tag{1}$$

$$25\,BaF_2-(40-2x)\,InF_3-(25+x)\,ZnF_2-(10+x)\,GdF_3 \quad \text{with } x=0-7 \tag{2}$$

These laws correspond to glasses whose composition is situated on two straight lines linking the most stable composition of the 10% GdF_3 diagram to the ones of the 15% diagram.

It is noteworthy that these empirical laws suggest that Gd^{3+} ions substitute for indium and zinc ions which are well-known glass formers. This is in accordance with previous results on RE fluorescence line-narrowing spectroscopy that showed that RE ions belong to the glass forming network [22].

The evolutions of glass stability as a function of gadolinium content $(10+x)$ in glasses (1) and (2) are shown in Fig. 6. In glass (1), the ΔT parameter ranges from 88°C for 10% GdF_3 ($x=0$) to a maximum of 95°C for 15% GdF_3. For concentration greater than 15%, the glass stability decreases. In glass (2), even though data are more scattered, the results indicate a maximum stability for $x=2.5$, which corresponds to an optimized GdF_3 concentration of 12.5%.

In a second stage, we have investigated the effect of GaF_3 substitution for InF_3 in BIZ–15% GdF_3 and BIZ–12.5% GdF_3 glasses.

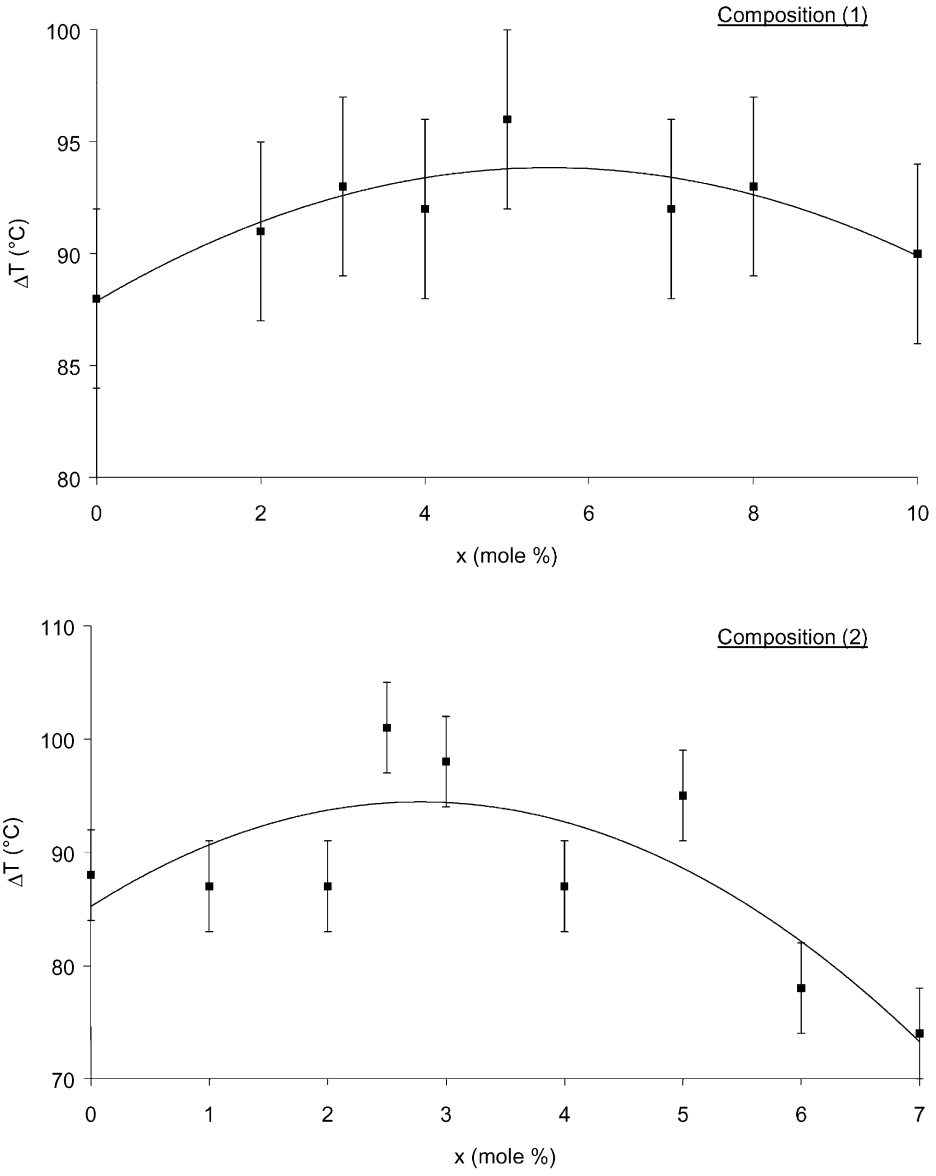

Fig. 6. Evolution of glass stability (ΔT) as a function of GdF_3 content $(10+x)$ in glass compositions (1) and (2). Lines are guide for the eye.

Table 4
Characteristic temperatures and stability parameter of BIZ–Gd–Ga glasses

Glass composition (mol%)					T_g (°C)	T_x (°C)	T_{peak} (°C)	ΔT (°C)
BaF_2	InF_3	ZnF_2	GdF_3	GaF_3				
25	35	25	15	0	309	405	408	96
25	30	25	15	5	315	433	440	118
25	27	25	15	8	319	447	456	128
25	25	25	15	10	322	450	459	128
25	24	25	15	11	323	463	479	140
25	23.5	25	15	11.5	324	460	471	136
25	23	25	15	12	324	469	478	145
25	22.5	25	15	12.5	324	458	469	134
25	22	25	15	13	326	464	477	138
25	20	25	15	15	329	444	451	115
25	35	27.5	12.5	0	302	403	414	101
25	32.5	27.5	12.5	2.5	306	420	426	114
25	31	27.5	12.5	4	310	414	419	104
25	30	27.5	12.5	5	311	421	430	110
25	29	27.5	12.5	6	310	423	429	113
25	27.5	27.5	12.5	7.5	312	429	437	117
25	25	27.5	12.5	10	314	430	437	116

Glasses with GaF_3 concentration from 0 to 15% and from 0 to 10%, respectively, were studied. The results are shown in Table 4.

First, it is observed that the glass transition temperature tends to increase with increasing GaF_3 content, which is in good agreement with previous results [23]. Second, addition of GaF_3 has a drastic effect on glass stability with a ΔT parameter as high as 145°C for BIZ–15% GdF_3–12% GaF_3. This is to be compared with $\Delta T = 96$°C for the base-glass. The stabilization effect is not as significant for BIZ–12.5% GdF_3–GaF_3. The maximum ΔT value is equal to 117°C for the glass containing 7.5% GaF_3. This corresponds to an improvement of 16°C only as compared to the base-glass.

As a result, the most stable composition at this stage is 25 BaF_2–23 InF_3–15 GdF_3–25 ZnF_2–12 GaF_3.

Substitution of glass modifiers NaF, SrF_2 and CaF_2 for another glass modifier, BaF_2, has been investigated. No stabilization effect was observed. Substitution of CdF_2 for BaF_2 in one hand and for ZnF_2 in the other hand have been also carried out. In the second case, valuable results have been obtained, as shown by the DSC curves of 6% CdF_2 glass and Cd-free glass in Fig. 7. It is observed that partial substitution of Cd for Zn results in a drastic flattening of the

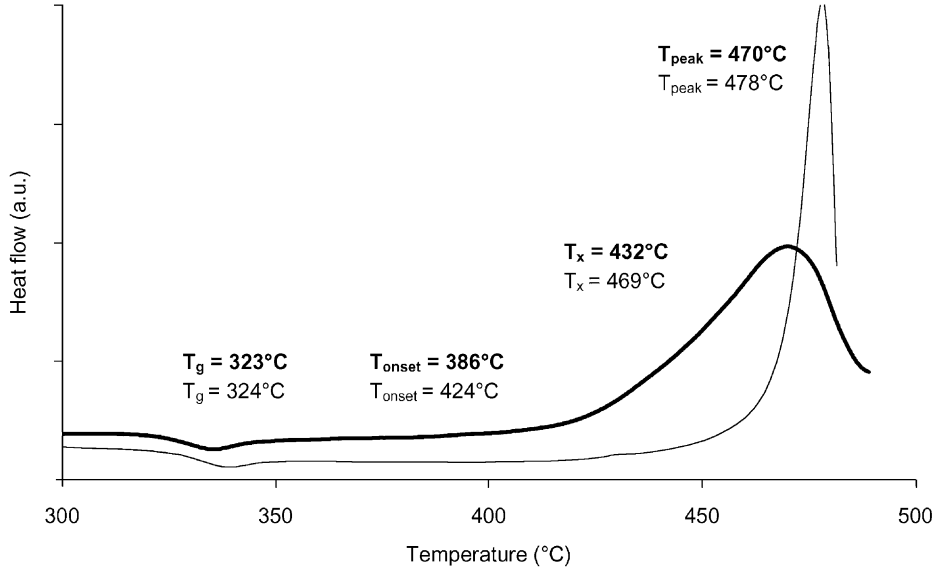

Fig. 7. DSC curves of 25 BaF_2–23 InF_3–25 ZnF_2–15 GdF_3–12 GaF_3 and 25 BaF_2–23 InF_3–19 ZnF_2–15 GdF_3–12 GaF_3–6 CdF_2 (bold) glasses. The curves are offset for better reading.

Table 5
Characteristic temperatures and stability parameter of $In_{40-x}Zn_{20}Sr_{20}Ba_{20}Ga_xF_{240}$ glasses

Glass composition (mol%)					T_g (°C)	T_x (°C)	T_{peak} (°C)	ΔT (°C)
InF_3	ZnF_2	SrF_2	BaF_2	GaF_3				
40	20	20	20	0	296	380	385	84
35	20	20	20	5	301	398	419	97
33	20	20	20	7	306	401	412	95
32	20	20	20	8	306	431	442	125
31	20	20	20	9	307	427	441	120
30	20	20	20	10	308	418	426	110
29	20	20	20	11	313	421	428	108
28	20	20	20	12	312	417	423	105
27.5	20	20	20	12.5	312	419	432	107
25	20	20	20	15	319	418	421	99

crystallization peak, which is indicative of lower kinetics of crystallization. However, the crystallization temperature is lower for the CdF_2 glass ($T_x = 432$°C), which leads to a stability parameter ΔT of 109°C. This is significantly less than the 145°C temperature difference measured for the Cd-free glass. Based on the crystallization peak shape, the 6% CdF_2 glass shows a lower tendency to crystallize in the 480°C region. On the other hand, this glass starts crystallizing at temperatures lower than that of the Cd-free glass, as shown by the values of T_x and T_{onset} temperatures. T_{onset} is defined as the temperature measured at the onset of the crystallization peak.

3.2. Glasses based on In, Zn, Sr and Ba fluorides.

In a first step, stabilization of the $In_{40}Zn_{20}Sr_{20}Ba_{20}F_{240}$ composition was realized by substitution of GaF_3 for InF_3. The results are shown in Table 5, in terms of characteristic temperature and stability parameter ΔT. Similarly to the BIZ–Gd family, addition of GaF_3 has a positive effect on glass stability with ΔT increasing by ≈40°C from the base-glass to the IZSB–8 GaF_3 composition.

As for the first family, substitution of (CaF_2 or NaF) for (BaF_2 or SrF_2) and substitution of CdF_2 for ZnF_2 have been carried out. None of those substitutions led to a significant improvement of ΔT. However, substitution of CaF_2 for BaF_2 resulted in glasses with flattened crystallization peak as shown in Fig. 8. The important point is that, contrary to BIZ–Gd glasses, no concomitant reduction of ΔT is observed. As a result, the 32 InF_3–20 ZnF_2–20 SrF_2–18 BaF_2–8 GaF_3–2 CaF_2 composition, referred to as IZSB–8 GaF_3–2 CaF_2 glass, represents the best compromise between high ΔT and low kinetics of crystallization in a temperature zone close to the fibering temperature. The infrared transmission of IZSB–8 GaF_3–2 CaF_2 glass is displayed in Fig. 9. The infrared cut-off is at around 7 μm as expected with glasses containing InF_3 and GaF_3. In the 3 μm region, a weak absorption band is observed. This is due to the presence of

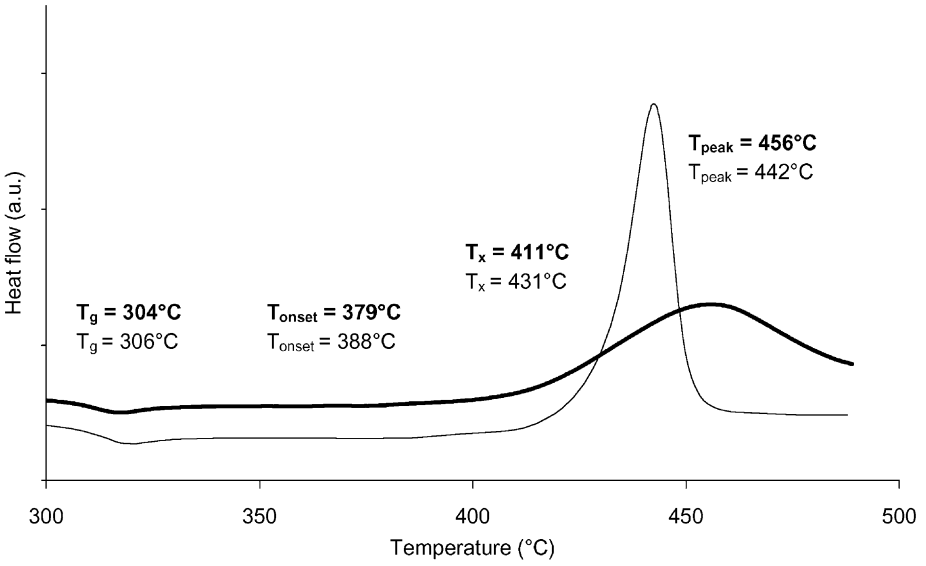

Fig. 8. DSC curves of composition 32 InF_3–20 ZnF_2–20 SrF_2–20 BaF_2–8 GaF_3 and 32 InF_3–20 ZnF_2–20 SrF_2–18 BaF_2–8 GaF_3–2 CaF_2 (glass). The curves are offset for better reading.

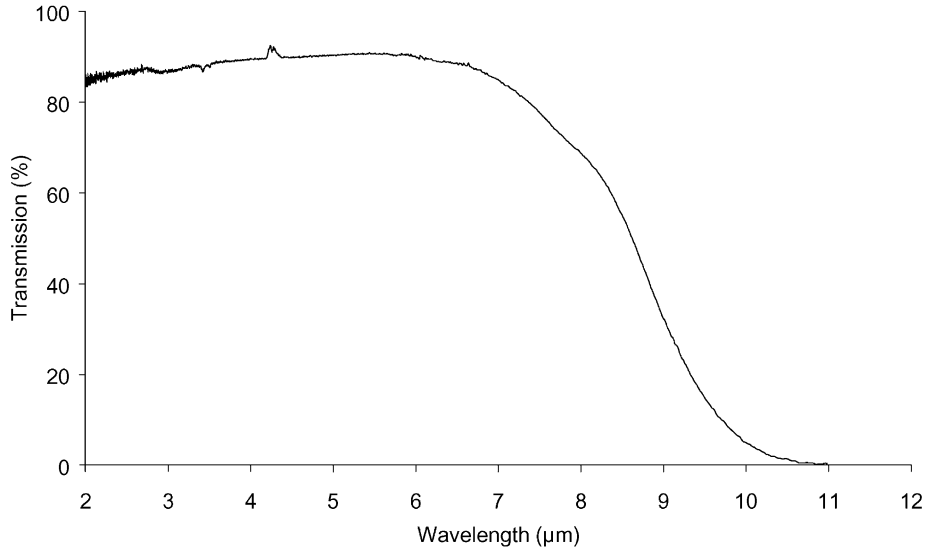

Fig. 9. Infrared spectra of the 32 InF_3–20 ZnF_2–20 SrF_2–18 BaF_2–8 GaF_3–2 CaF_2 glass ($e = 3$ mm).

residual OH^- hydroxyl ions in the glass. Thorough glass preparation under reactive atmosphere such as NF_3 results in the removal of OH^- traces.

Fibrability of the most stable glass compositions was investigated, that is of

$$BIZ-15\,GdF_3-12\,GaF_3 \quad (3)$$

$$BIZ-15\,GdF_3-12\,GaF_3-6\,CdF_2 \quad (4)$$

$$IZSB-8\,GaF_3 \quad (5)$$

$$IZSB-8\,GaF_3-2\,CaF_2 \quad (6)$$

Fibers were pulled from glass rods of 60–80 mm in length and 9 mm in diameter with a classical fiber-drawing tower. The drawing temperature, measured at a distance of 10 mm from the surface of the glass rod in the heating chamber, was 410°C. At this temperature, fiber pulling had to be initiated manually. The temperature was maintained as low as possible during the experiment in order to avoid surface crystallization of the glass.

However, glasses (3), (4), and (5) lead to short fibers with significant crystallization. On the other hand, up to 5 m of glass fibers with no visible crystallization could be obtained from glass (6), IZSB–8 GaF_3–2 CaF_2.

This experimental result is in good accordance with the DSC curves in Figs. 7 and 8 where it is observed that glass (6) presents the best compromise between low kinetics of crystallization and high onset temperature for crystallization with respect to T_g.

4. Experimental methods

Glass samples were prepared from metal fluorides and oxides, whose chemical purity and origin are listed in Table 6.

Table 6
Chemical purity and origin of starting materials

Product	Chemical purity	Origin
BaF_2	4N	Alfa
SrF_2	4N	Cerac
ZnF_2	3N	Alfa
Ga_2O_3	3N	Alusuisse
Gd_2O_3	3N	Rhone–Poulenc
In_2O_3	4N	Metaleurop

For routine preparation, starting materials were mixed carefully with a fluorinating agent, NH_4HF_2 (3N) from Cerac. Fluorination was carried out in air in a platinum crucible at 320°C for about 3 h. In a second step, the excess of NH_4HF_2 was eliminated for 1 h at 500°C.

Then, the mixture was melted at 900°C for 5 min and poured into a brass mold at room temperature. Samples (40 mm × 20 mm × 3 mm) were obtained.

Most stable compositions were prepared in a glove box filled with dry argon in order to avoid contamination by atmospheric moisture. The melts were poured in a mold preheated at a temperature close to the glass transition temperature. Characteristic temperatures were measured with a Setaram DSC 131 equipment with experimental errors of ±2°C.

Infrared transmission spectra were recorded by using a Bomem M100 FTIR spectrometer.

5. Conclusion

In summary, we have reviewed the thermal and optical properties of fluoride glasses suitable for waveguide applications, either fibers or planar waveguides. It was reported that fluoride glasses doped with Pr^{3+} and Tm^{3+} rare-earth

ions are valuable solutions for optical amplification in the 1.3 and 1.47 μm telecommunication band.

Then, we have presented results on the synthesis and characteristics of optimized fluoride glasses based on indium fluoride. Glasses were investigated in the (Ba, In, Zn, Gd) and (In, Zn, Sr, Ba) fluoride systems. Further improvement of the glass stability was achieved by addition of other elements such as: Ga, Cd, Ca. Most stable glasses showed a stability parameter ($T_x - T_g$) as high as 145°C. Fibrability was demonstrated only for glasses belonging to the second system and stabilized by incorporation of gallium and calcium fluorides. This result is in good agreement with DSC data.

Acknowledgements

This work has been supported by ''Reseau National de Recherche en Telecommunication''.

References

[1] D. Hewak (Ed.), Properties, processing and applications of glass and rare-earth-doped glasses for optical fibres, EMIS Datareviews series no. 22, INSPEC, London, 1998, pp. 159–279.
[2] J.L. Adam, J. Lucas, S. Jiang, SPIE 2996 (1997) 8–17.
[3] P.A. Tick, SPIE 2287 (1994) 47–57.
[4] J.L. Adam, in: T. Nakajima, A. Tressaud, B. Zemva (Eds.), Advanced Inorganic Fluorides: Synthesis, Characterization and Applications, Elsevier, Amsterdam, 2000, pp. 235–282 (Chapter 8).
[5] D. Szebesta, S.T. Davey, J.R. Williams, M.W. Moore, J. Non-Cryst. Solids 161 (1993) 18–22.
[6] E. Desurvire, Phys. Today January (1994) 20–27.
[7] M. Dejneka, B. Samson, Mater. Res. Soc. Bull 24 (1999) 39–45.
[8] E. Josse, J.E. Broquin, E. Lebrasseur, G. Fonteneau, R. Rimet, B. Jacquier, J. Lucas, SPIE 2996 (1997) 74–85.
[9] W. Seeber, E.A. Downing, L. Hesselink, M.M. Fejer, D. Ehrt, J. Non-Cryst. Solids 189 (1995) 218–226.
[10] J. Lucas, J. Fluorine Chem. 72 (1995) 177–181.
[11] C. Jacoboni, O. Perrot, B. Boulard, J. Non-Cryst. Solids 184 (1995) 184–189.
[12] Y. Miyajima, T. Komukai, T. Sugawa, T. Yamamoto, Opt. Fiber Technol. 1 (1994) 35–47.
[13] Y. Ohishi, in: Proceedings of XVI International Congress on Glass, Beijing, China, 1995, pp. 115–122.
[14] B.J. Ainslie, S.T. Davey, D. Szebesta, J.R. Williams, M.W. Moore, T. Whitley, R. Wyatt, J. Non-Cryst. Solids 184 (1995) 225–228.
[15] A. Jha, B.E. Kinsman, E.R. Taylor, G. Kakarantzas, J. Non-Cryst. Solids 213/214 (1997) 101–105.
[16] A. Brenier, C. Pedrini, B. Moine, J.L. Adam, C. Plédel, Phys. Rev. 41 (1990) 5364–5371.
[17] T. Kasamatsu, Y. Yano, H. Sekita, Electron. Lett. 36 (2000) 1607–1609.
[18] D. Bayart, P. Baniel, A. Bergonzo, J.Y. Boniort, P. Bousselet, L. Gasca, D. Hamoir, F. Leplingard, A. Le Sauze, P. Nouchi, F. Roy, P. Sillard, Electron. Lett. 36 (2000) 1569–1571.
[19] B. Clesca, D. Bayart, L. Hamon, J.L. Beylat, C. Coeurjolly, L. Berthelon, Electron. Lett. 30 (1994) 586.
[20] A. Bouaggad, Ph.D. thesis, University of Rennes, 1986.
[21] Y. Messaddeq, A. Delben, M. Boscolo, M.A. Aegerter, A. Soufiane, M. Poulain, J. Non-Cryst. Solids 161 (1993) 210–212.
[22] J.L. Adam, V. Ponçon, J. Lucas, G. Boulon, J. Non-Cryst. Solids 91 (1987) 191–202.
[23] J. Lucas, I. Chiaruttini, G. Fonteneau, P. Christensen, S. Mitachi, SPIE 1228 (1990) 56–62.